JOURNAL OF MATERIALS SCIENCE 22 (1987) 3118–3128

Non-destructive ultrasonic evaluation of $CaCO_3$-filled polypropylene mouldings

B. BRIDGE, K. H. CHENG
Department of Physics, Brunel University, Kingston Lane, Uxbridge, Middlesex, UB8 3PH, UK

The dynamic elastic moduli and Poisson's ratio of calcium carbonate-filled polypropylene mouldings have been determined for a continuous range of filler loadings of between 0 and 40% volume fraction. Measurements were made non-destructively on bulk samples in the form of plates 2 cm × 2 cm square and 3 mm thick, at 5 MHz. The composition dependences of the elastic properties are compared with the Hashin and Shtrikman bounds for two-phase materials. All data were in close correspondence with the lower bound, suggesting that the fill particles were well dispersed, relatively free of agglomeration, well bonded to the matrix, and that particle sizes were much less than $\lambda/4$, i.e. much less than 100 μm, where λ is the wavelength of compressional waves.

1. Introduction

The potential of ultrasonic methods for the non-destructive inspection of filled polymers is so great that it is surprising how few inroads in this direction have yet been made. There are, of course, numerous ways to use ultrasound for materials evaluation because of the complexity of its interaction with atomic and molecular systems and structural inhomogeneities. Several of these methods are applicable to filled polymers. By devising appropriate experiments, it is feasible to determine the size, shape and distribution of filler particles, to detect agglomeration, to study the quality of the filler–matrix interface (i.e. the bonding), to evaluate stress distributions [1, 2], and detect microporosity. Most of the structural characterizations so obtained, with the possible exception of residual stress analysis, are done very well already by a combination of techniques such as SEM, electron spectroscopy for chemical analysis (ESCA), optical microscopy, X-ray and neutron diffraction, ashing, etc. However, these methods have to be performed on sections, fracture surfaces, or by other destructive means. Alternatively, non-destructive surface analysis techniques are clearly restricted by the "skin effects" present in mouldings. In contrast, ultrasonic evaluation, apart from being non-destructive, can be performed on large polymer samples, several millimetres to several centimetres thick, with no limit in principle on the cross-sectional area of the sample. In this context the only competitors to ultrasonic technique are radiography and thermography, methods which the authors are evaluating in parallel with the ultrasonic approach.

2. Theoretical considerations

The present report concerns perhaps the simplest of all ultrasonic evaluation techniques for filled polymers, i.e. comparison of the composition dependence of experimental (dynamic) elastic moduli with theoretical bounds. For quasi-statically applied stresses the well-known formulae of Hashin and Shtrikman [3–7], for the bounds for bulk and shear moduli of a two-phase material in which the second phase is in the form of particles, are

$$K_L = K_2 + (1 - V_2) \Big/ \left(\frac{1}{K_1 - K_2} + \frac{3V_2}{3K_2 + 4G_2} \right) \qquad (1)$$

$$G_U = G_2 + (1 - V_2) \Big/ \left(\frac{1}{G_1 - G_2} + \frac{6(K_2 + 2G_2)V_2}{5G_2(3K_2 + 4G_2)} \right) \qquad (2)$$

$$K_L = K_1 + V_2 \Big/ \left(\frac{1}{K_2 - K_1} + \frac{3(1 - V_2)}{3K_1 + 4G_1} \right) \qquad (3)$$

$$G_L = G_1 + V_2 \Big/ \left(\frac{1}{G_2 - G_1} + \frac{6(K_1 + 2G_1)(1 - V_2)}{5G_1(3K_1 + 4G_1)} \right) \qquad (4)$$

where the subscripts U and L denote upper and lower bounds, respectively, subscripts 1 and 2 denote the matrix and the particulate phase, respectively, and V is the volume fraction.

It is noteworthy that these bounds are not independent, since they are obtained merely by reversing the roles of matrix and filler in the analysis. Equivalent upper and lower bounds for the longitudinal modulus, L, Young's modulus, E, and Poisson's ratio, σ, are obtained simply by combining Equations 1 to 4 with the well-known relationships

$$L = K + \tfrac{4}{3}G \qquad (5)$$

$$G = E/2(1 + \sigma) \qquad (6)$$

$$K = EG/3(3G - E) \qquad (7)$$

The Hashin and Shtrikman bounds apply for an arbitrary size and shape distribution of particles provided only that there are many particles in the volume element (the averaging volume) over which

0022–2461/87 $03.00 + .12

mean moduli are measured, and that the particle dimensions are small compared with the dimensions of the volume element. When the particles are spherical, the lower bound actually becomes exact, irrespective of the particle distribution. When the particles are not negligible compared with the volume element mentioned hitherto, wider bounds on the elastic moduli hold. Thus, when the second phase is in the form of layers parallel to or perpendicular to the axis of strain, the Voigt and Reuss bounds [5, 6] hold respectively, i.e.

$$K_V = (1 - V_2)K_1 + V_2K_2 \tag{8}$$

$$G_V = (1 - V_2)G_1 + V_2G_2 \tag{9}$$

$$\frac{1}{K_R} = \frac{1 - V_2}{K_1} + \frac{V_2}{K_2} \tag{10}$$

$$\frac{1}{G_R} = \frac{1 - V_2}{G_1} + \frac{V_2}{G_2} \tag{11}$$

For long fibres running parallel to, or perpendicular to the strain axis, bounds in between the Hashin and Shrikman bounds at one extreme, and the Voigt and Reuss bounds at the other, will hold.

So far we have talked only about quasi-statically applied stresses but we are concerned with ultrasonically applied stresses, and corresponding dynamic measurements of G and K from the bulk and shear wave propagation velocities, C_L and C_T respectively, as given by

$$C_L = \left(\frac{(4G/3) + K}{\varrho}\right)^{1/2} \tag{12}$$

$$C_T = \left(\frac{G}{\varrho}\right)^{1/2} \tag{13}$$

where ϱ is the mean sample density.

In ultrasonic propagation the stress and strain vary spatially and the dynamic elastic moduli are determined by the ratio of these quantities at a "point," i.e. the averaging volume has dimensions small compared with wavelength λ in the propagation direction. It follows that provided the filler particles have dimensions very much smaller than a wavelength in the propagation direction, we might reasonably expect the bounds on the dynamic moduli to be given by Equations 1 to 4, and 8 to 11, derived for the quasi-static case. An alternative way of expressing the same idea is to say that if particle sizes are not negligible compared with λ (more stringently $\lambda/4$), interference effects between incident and scattered waves will take place at each filler–matrix boundary [7–9]. This will cause elastic moduli to be a function of the wavelength and particle dimensions, an effect which is not predicted by the Hashin and Shtrikman "quasi-static" boundary conditions. Thus it is interesting to note that large agglomerates in a material nominally expected to contain a uniform dispersion of spherical particles of size much less than $\lambda/4$ will show up as a deviation of the elastic moduli from the lower Hashin and Shtrikman bound. If unusual residual stress distributions at the filler–matrix interface violate the boundary conditions implicit in the Hashin and Shtrikman theory, deviations of experimental moduli from the theoretical bounds might again be expected. This tempts us to add that in static modulus measurements the strain levels are such that irreversible deformations take place, and it is doubtful whether the theory is applicable anyway in this case. Ultrasonic measurements are performed at very small and reversible strain levels – probably giving much better prospects for the theory to agree with experiment when particle sizes are appropriate.

For our first experiments the $CaCO_3$–polypropylene system was chosen because it is of some practical interest. Filler particle sizes of micrometre size, to meet the above-mentioned "wavelength" constraint, are readily obtained.

3. Experimental sample preparation and ultrasonic measurements

The polypropylene used was supplied by Polypropylene Marketing, ICI Plastics Divisions, Welwyn Garden City, Hertfordshire, UK. It was in the form of powder under the trade name "Propathene GW522M" and was of density 0.905 g cm^{-3}. The calcium carbonate was supplied by OMYA (Brohler Strasse II, 5000 Köln 51, FRG). It was a fine, white, high purity filler under the trade name "Millicarb" and of density 2.7 g cm^{-3}.

rigged with two hoppers. The matrix and filler were contained separately in the two hoppers, and by adjusting the relative feed rates of the hoppers, batches of polypropylene filled with varying volume fractions of calcium carbonate were produced. The extruded strips were granulated and then compressed into sheets of dimensions 2 mm × 10 cm × 10 cm and 3 mm × 10 cm × 10 cm. Small samples of area 2 cm × 2 cm were then cut out of each plastic sheet to study the deviation of composition within each sheet and special care was taken to exclude the voids which were inevitably present near the edges of the compressed plastic sheets (see Fig. 1).

By calibrating the throughput rates of the two hoppers, the volume fractions of the constituents in the extruded plastic could be calculated. However, the values of volume fractions obtained in such a way were far from reliable due to the fluctuation in the feeding rates of the hoppers and the inherent inadequacy in the mixing power of the extrusion machine.

More accurate determination of the compositions of the filled plastic was achieved by considering the fact that the volume of a composite material, with no chemical reaction between the two phases, is the sum of the volumes of the constituents. It is easy to derive that the volume fraction of the filler phase (V_2) is given by

$$V_2 = \frac{\varrho - \varrho_1}{\varrho_2 - \varrho_1} \tag{14}$$

using the same subscripts as previously.

Since the densities of the matrix and filler were available from the suppliers' information, only the density of each sample was required to determine the volume fractions of the two phases. This was done by measurements using the Archimedes method in which a sample was first weighed in air, and then in a suitable liquid. Distilled water was used in the measurements

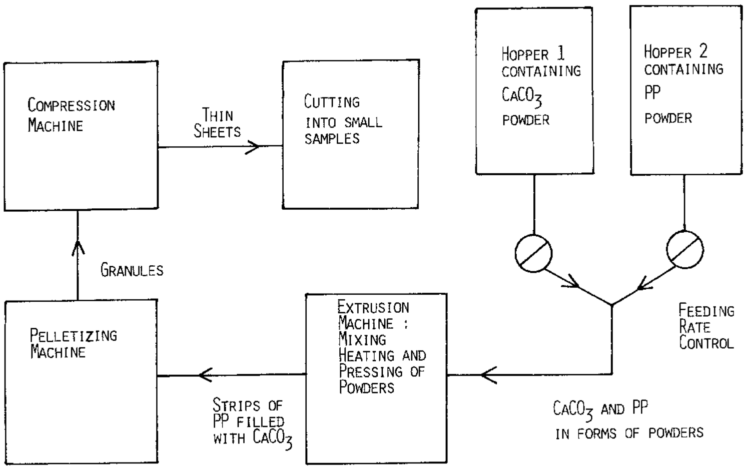

Figure 1 Preparation of samples for off-line testing.

for the samples of densities greater than unity and methanol was used for those with lower densities. The following calculation yields the required density (ϱ):

$$\varrho = \frac{\text{(weight in air)}}{\text{(weight in air)} - \text{(weight in suitable liquid)}} \times \text{(density of the liquid)} \qquad (15)$$

Ultrasonic pulse echoes were propagated through the 2 cm × 2 cm faces by the use of broad-band pulser–receiver (Panametrics, USA, Model 5052PR) and 5 MHz broad-band contact probes (12.5 mm diameter compressional from Ultrasonoscope Ltd, UK, and 5 mm diameter shear Model V156 Serial No. 48133 from Panametrics). Echoes were displayed on a broad-band oscilloscope (Tetronix Model 2445, 150 MHz). Time differences between any two points of interest in the echo trace were measured by a high-performance digital delay generator (Berkeley Nucleonics, USA, Model 7030). Techniques for velocity measurement by using the first quarter-cycle of r.f. above the noise as a reference in each echo of interest, has been described elsewhere [10–12]. Coupling fluids used were Nonaq stopcock grease (G-530) for compressional waves and a clear thixotropic fluid (P3-7570 from Telidictor, UK, Ltd.) for shear measurements.

Measurement of the time lag between successive echoes was only possible for the determination of compressional velocity. The attenuation of shear waves by the plastic material being studied was so great that the second echo was barely distinguishable from the background noise. Another technique known as the velocity comparison method was therefore employed for shear velocity determination. Shear waves were first propagated into a reference block and, by manipulating the time-base setting of the oscilloscope and the delayed trigger pulse from the digital delay generator, only the first echo was displayed and made to occupy the full screen of the oscilloscope so as to increase the measurement accuracy. Without altering the settings of the instruments, shear waves were then sent into the sample and the shift in position of the first echo was noted.

The shear velocity in the sample was given by the following expression:

$$t_r - t_p = t_s$$

$$t_r - \frac{2d}{V_p} = t_s$$

$$V_p = \frac{2d}{t_r - t_s}$$

where t_r = travel time of shear waves in the reference block, t_p = travel time of shear waves in the plastic sample, t_s = shift in position in terms of time and d = thickness.

The essential feature of the whole measuring system is the programmable digital delay generator (Model 7030 from Berkeley Nucleonics Corporation, 1198 Tenth Street, California 94710).Precise delay controls are obtained by counting pulses from a built-in 100 MHz oscillator for a preset period of time which is determined by the front panel switches. An input signal triggers a counter to start and, after a predetermined number of clock pulses has been counted, delayed data are accepted. This unit combined with the trigger selector to allow any part of the oscilloscope trace to be observed and its time relative to the delay pulse to be measured absolutely to ± 0.5 nsec or 0.01%, depending on which one is greater. Small travel-time differences between different samples, however, can be measured to a much greater precision of 100 psec, which is the time jitter of the digital delay pulse. In this way, a precision of 1 in 10^5 could be obtained in the travel-time measurements for the purposes of sample comparison.

The thicknesses of the samples were measured by using a micrometer with an accuracy of ± 0.005 mm. For compressional velocity determination, thicknesses of several points on a sample within the ultrasonic probe contact area were measured and the mimimum of the thicknesses was used to calculate the compressional velocity. On the other hand, due to the relatively small diameter of the shear-wave probe used, the central thickness of a sample was used for the shear velocity calculation.

It will be evident from the previous discussions on the time measurement equipment and density measurements that the accuracies of ultrasonic wave velocity and elastic modulus measurements are determined solely by the tolerances on the sample thicknesses. These tolerances in turn were fixed entirely by the moulding technology: quite deliberately we decided against grinding and polishing the samples to optical parallelism since we could then hardly claim to have a practical, viable, non-destructive evaluation technique, given the time-consuming nature of such preparations.

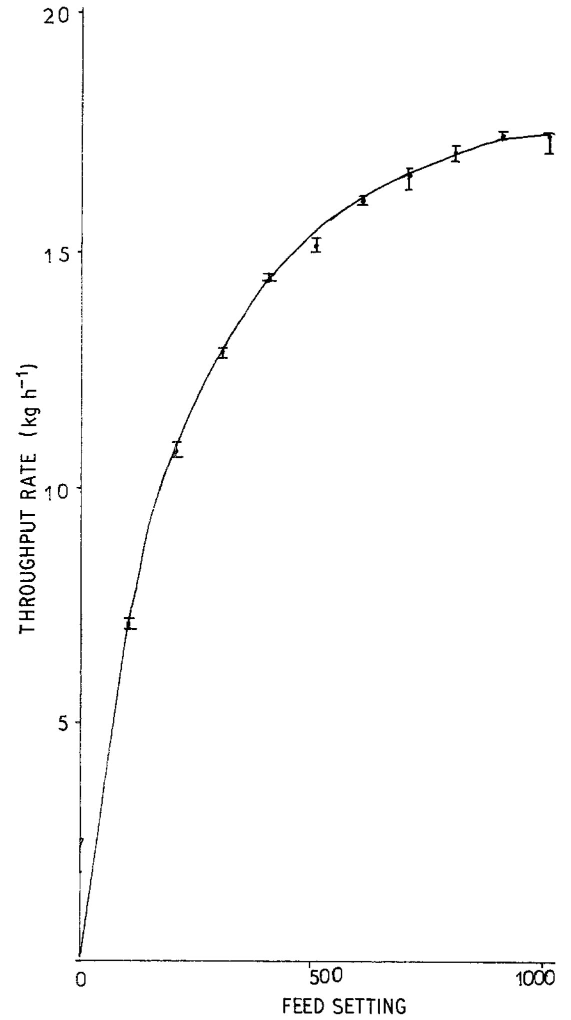

Figure 2 Calibration of the Plasticolor Proportioning Unit (with conveyor screw 17/25) containing polypropylene powder GW522M. At various feed settings of the hopper, ten measurements of the throughput rates were made. The maximum, mean and minimum of ten measurements at each feed setting were determined and are indicated by the error bars.

4. Results

Two hoppers were used for feeding the extrusion machine, namely the Plasticolor Proportioning Unit with conveyor-screw 17/25 for the polypropylene powder (Woywod Plaststore, Wendelsteinstrasse 6 8032, Grafelfing, FRG) and a feeder (K-Tron-Soder, AG, 5702 Niederlenz, Schweiz Suisse, Switzerland) for the calcium carbonate powder. The feeding rates of materials were calibrated against the settings of the hoppers and the results are given in Figs 2 and 3.

Having done the calibration, samples of different compositions were obtained by varying the relative feeding rates of the hoppers and the theoretical compositions obtainable are given by the straight line in Fig. 4. Also shown in Fig. 4 are the mean, maximum and minimum of the actual compositions, determined by measuring the densities of the samples, resulting from various settings of the hoppers. These give a reliable indication of the scattering within a particular, nominally uniform composition.

It is clear from Fig. 4 that the deviation of the actual compositions from the expected compositions, as well as the variation within a nominally uniform composition, increase towards both low and high calcium carbonate ($CaCO_3$) concentration regions. This can be attributed to the increased significance of the fluctuation in feedings rates of the hoppers at low $CaCO_3$ content and the inadequacy in mixing efficiency of the extrusion machine at high $CaCO_3$ content. Nevertheless, the hoppers seem to give a fairly good control on the extrudate composition over the range from 7 to 25% by volume of $CaCO_3$.

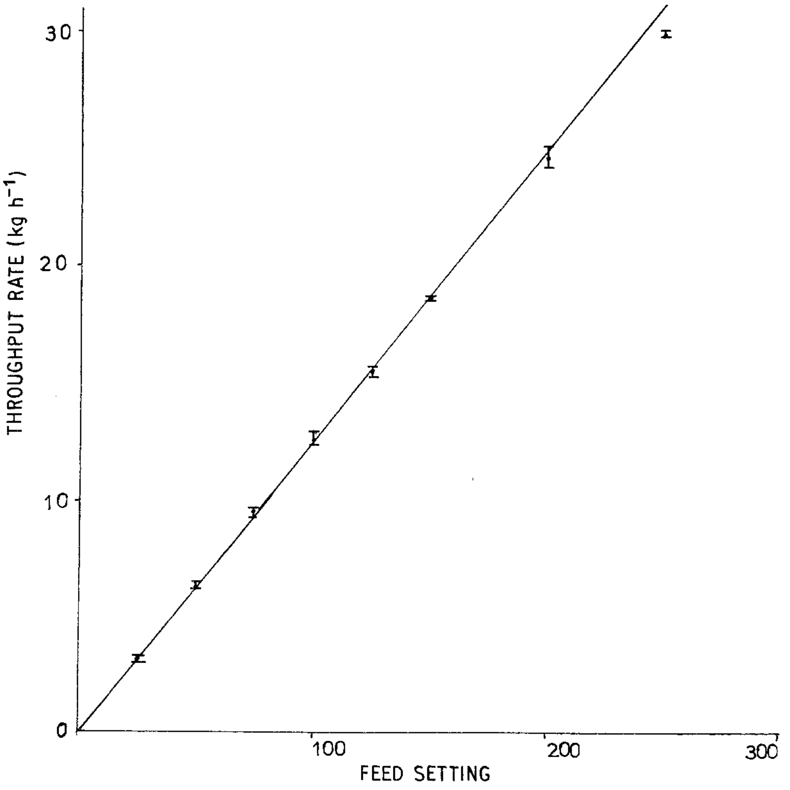

Figure 3 Calibration of the feeder for $CaCO_3$ powder. At various settings of the hopper ten measurements of the throughput rates were made. The maximum, mean and minimum of the measurements at each feed setting are indicated by the error bars.

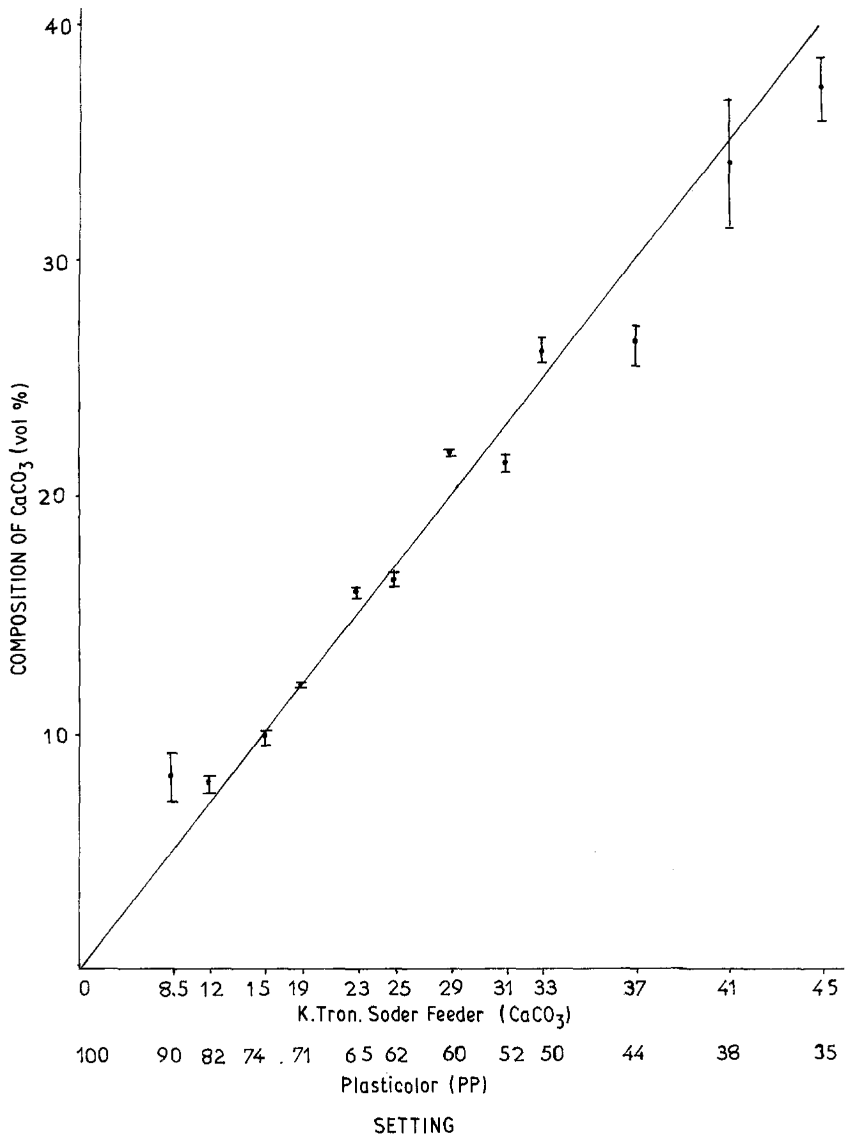

Figure 4 The straight line represents the theoretical compositions obtainable from the settings of the hoppers indicated on the *X* axis. The maximum, mean and minimum of the actual compositions of the samples produced at each pair of setttings are also indicated by the error bars.

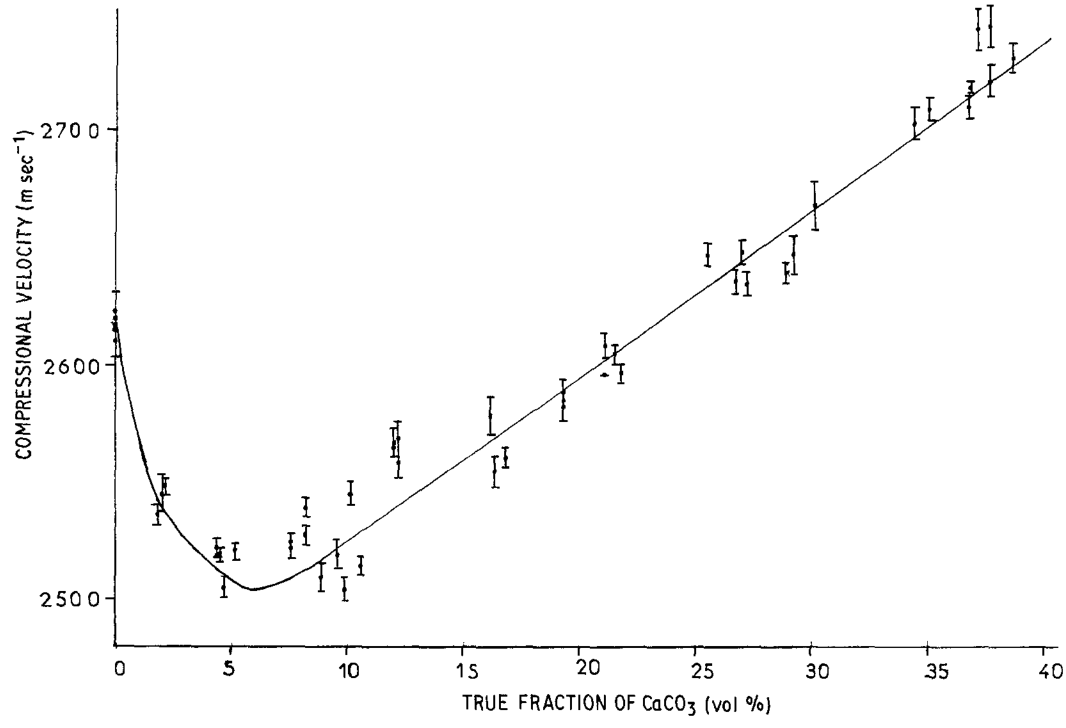

Figure 5 Composition dependence of compressional wave velocities. Error bars indicate means and standard deviations. True volume fraction of CaCO$_3$ determined by density measurement.

TABLE I Sample preparation and measurements

Batch No./ Sample No.	Nominal fraction of $CaCO_3$ (vol %)	Density ($g\,cm^{-3}$)	True fraction of $CaCO_3$ (vol %)*	Thickness (mm)		Compressional velocity ($m\,sec^{-1}$)		Shear velocity ($m\,sec^{-1}$)		Mean shear modulus (GPa)	Mean bulk modulus (GPa)	Mean Poisson's ratio	Mean Young's modulus (GPa)
				Minimum	Centre	Mean	Standard deviation	Mean	Standard deviation				
7/129	0.1	0.905	0	2.875	2.905	2623	7	1270	8	1.46	4.28	0.3468	3.933
7/130				2.960	2.985	2618	8	1255	4	1.425	4.303	0.3508	3.850
7/131				3.060	3.060	2611	10	1254	5	1.425	4.272	0.3501	3.842
7/132				2.825	2.835	2618	7	1256	3	1.428	4.305	0.3506	3.857
7/132				2.880	2.900	2623	10	1266	6	1.451	4.323	0.3491	3.915
7/134				3.000	3.020	2620	11	1263	7	1.444	4.278	0.3483	3.894
47/141	1.0	0.938	1.8	2.130	2.130	2536	4	1216	6	1.387	4.169	0.3502	3.746
47/142		0.941	2.0	2.190	2.190	2545	8	1213	5	1.385	4.191	0.3530	3.748
47/143		0.942	2.1	2.100	2.100	2549	3	1217	10	1.395	4.201	0.3524	3.733
48/144	3.0	0.987	4.5	2.200	2.210	2519	3	1216	10	1.459	4.413	0.3511	3.943
48/145		0.984	4.4	2.160	2.170	2522	4	1207	7	1.433	4.412	0.3535	3.879
48/146		0.990	4.7	2.220	2.240	2505	4	1214	7	1.459	4.267	0.3465	3.929
48/147		0.998	5.2	2.205	2.225	2521	4	1217	6	1.478	4.372	0.3481	3.985
49/148	5.0	1.083	9.9	2.165	2.180	2504	5	1235	6	1.652	4.580	0.3390	4.424
49/149		1.077	9.6	2.270	2.305	2519	6	1238	9	1.650	4.634	0.3408	4.425
49/150		1.095	10.6	2.275	2.300	2514	4	1243	8	1.692	4.665	0.3382	4.529
49/151		1.065	8.9	2.350	2.380	2509	5	1222	10	1.590	4.584	0.3382	4.529
16.54	7.0	1.053	8.2	2.865	2.900	2527	4	1257	8	1.664	4.506	0.3445	4.276
16/55		1.041	7.6	2.730	2.750	2522	3	1260	10	1.653	4.417	0.3356	4.445
16/56		1.043	7.7	2.675	2.715	2524	3	1259	10	1.653	4.440	0.3336	4.409
16/57		1.053	8.2	3.005	3.025	2539	4	1250	7	1.645	4.505	0.3344	4.412
21/71	10.0	1.087	10.1	2.950	2.970	2545	5	1260	8	1.726	4.739	0.3400	4.409
23/75	12.0	1.121	12.0	3.000	3.025	2567	6	1272	9	1.814	4.968	0.3376	4.617
23/76		1.121	12.0	3.000	3.015	2566	5	1279	11	1.834	4.936	0.3372	4.851
23/77		1.123	12.1	3.070	3.080	2569	7	1271	8	1.814	4.993	0.3347	4.896
23/78		1.123	12.1	2.990	3.000	2558	6	1277	11	1.831	4.887	0.3379	4.854
29/84	17.0	1.207	16.6	2.990	3.020	2561	4	1306	10	2.059	5.171	0.3335	4.883
29/85		1.200	16.4	2.820	2.845	2555	6	1311	8	2.062	5.084	0.3242	5.453
29/86		1.196	16.2	2.845	2.860	2579	8	1305	10	2.037	5.239	0.3279	5.410
34/102	23.0	1.284	21.1	3.060	3.100	2597	1	1342	8	2.312	5.577	0.3179	6.094
34/103		1.290	21.5	2.985	3.025	2605	4	1337	7	2.306	5.679	0.3212	6.094
34/104		1.287	21.8	2.300	3.070	2597	4	1327	7	2.284	5.702	0.3233	6.045
34/105		1.284	21.1	2.380	3.150	2609	5	1346	10	2.326	5.639	0.3187	6.135
38/115	30.0	1.385	26.7	2.234	2.250	2636	5	1378	13	2.630	6.117	0.3120	6.901
38/116		1.394	27.2	2.295	2.320	2635	5	1374	12	2.632	6.170	0.3133	6.913
38/117		1.389	27.0	2.300	2.330	2648	5	1377	7	2.634	6.228	0.3147	6.926
38/118		1.363	25.5	2.380	2.410	2647	5	1376	9	2.581	6.109	0.3148	6.787

41/121	35.0	1.566	36.8	2.250	2.260	2709	4	1390	8	3.211	7.211	0.3061	8.388
41/122		1.564	36.7	2.325	2.340	2710	5	1404	13	3.153	7.282	0.3108	8.266
45/15	40.0	1.597	38.6	2.420	2.425	2731	6	1439	16	3.307	7.502	0.3078	8.650
45/16		1.580	37.6	2.335	2.350	2720	7	1437	9	3.263	7.339	0.3064	8.526
45/18		1.570	37.1	2.320	2.330	2743	8	1437	7	3.242	7.473	0.3309	5.627
28/87	17.0	1.251	19.3	2.255	2.275	2586	4	1300	8	2.114	5.547	0.3279	5.702
28/89		1.251	19.3	2.130	2.130	2589	4	1310	10	2.147	5.523	0.3321	5.595
28/90		1.252	19.3	2.100	2.100	2583	5	1295	12	2.100	5.553	0.3107	7.215
39/119	30.0	1.430	29.2	3.090	3.105	2647	8	1387	9	2.751	6.351	0.3195	7.199
39/120		1.445	30.1	3.205	3.205	2668	10	1374	9	2.728	6.649	0.3203	6.852
35/110	25.0	1.424	28.9	2.260	2.260	2640	4	1350	8	2.595	6.355	0.3203	6.852
44/10	40.0	1.522	34.4	3.030	3.100	2703	7	1433	4	3.125	6.953	0.3046	8.154
44/14		1.533	35.0	3.025	3.040	2709	5	1441	3	3.183	7.006	0.3028	8.294

*Volume fraction determined by density measurement.

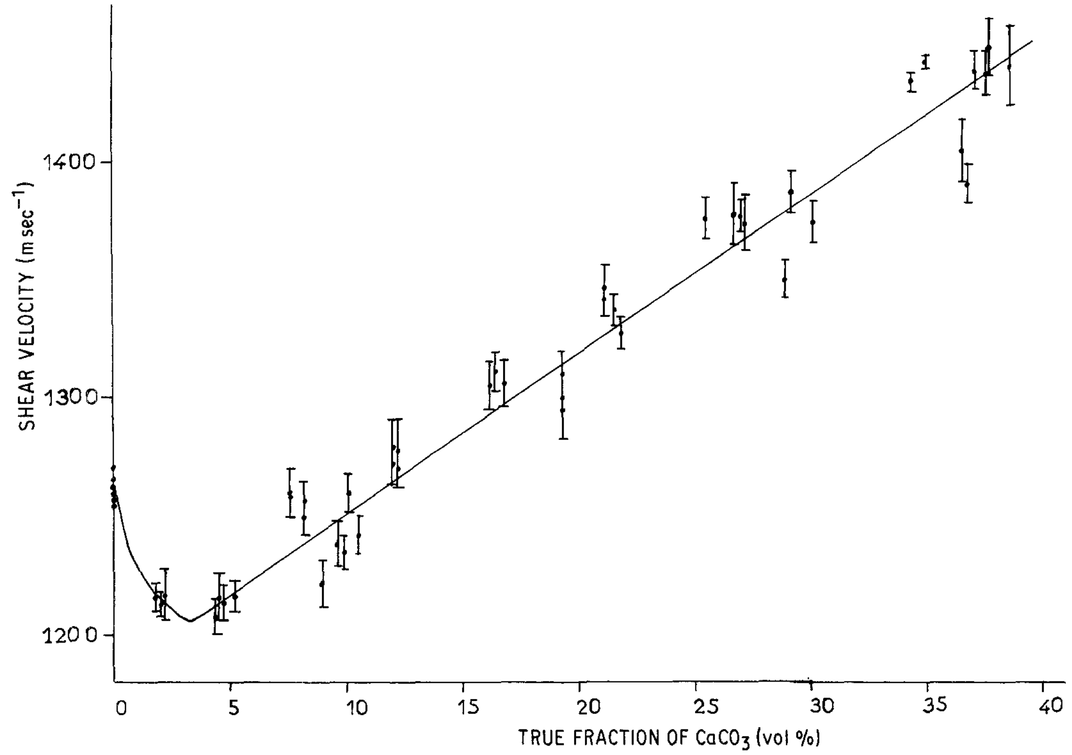

Figure 6 Composition dependence of shear wave velocity.

It will be observed that the standard deviations in the velocity measurement data are of the same order as the error in the thickness measurements (± 0.2%), confirming that the prevision time-of-fight technique employed added little to the thickness measurement above. A complete history of the sample preparation and measurements performed is given in Table I. Even though some of the data contained therein are repeated in subsequent figures, this table gives a convenient summary of the potential of ultrasonic measurements as a non-destructive evaluation technique, since all the errors and standard deviations at each measurement stage are contained here. Of particular interest is the tolerance on the sample thicknesses as this is the weakest part of the whole technique.

Figs 5 and 6 show, respectively, the experimentally determined relationships between the compressional and shear velocities and the compositions of the samples. Both graphs show a common trend. The addition of $CaCO_3$ causes an initial decrease of velocity, followed by an increase. The minimum compressional velocity occurs at about 6 vol % $CaCO_3$ while the minimum shear velocity occurs at about 3 vol %. In the graphs, every point represents the mean value of five independent measurements on an individual sample, i.e. measurements made with five different probe-specimen bonds. Five repeated measurements on each sample should give a good indication of the reproducibility of the experimental results. The standard deviation of the five measurements was calculated for each sample and is represented by an error bar associated with each experimental point. For compressional velocity measurements, the maximum and mean of the standard deviations among all the samples were found to be 11 and 6 m sec^{-1}, respectively, while those for shear velocity measurements were respectively 16 and 8 m sec^{-1}.

From velocities and densities of the samples, the elastic moduli were calculated by manipulating Equations 5 to 7, 12 and 13. For every sample, five values of the respective moduli were obtained but, for the sake of clarity, only the mean of the five values was plotted in Figs 7 to 10. No error bars were drawn in the graphs but the maximum and mean of the standard deviations among the samples should give a good indication of the reproducibility of the results (as shown in Table II).

Also shown in Figs 7 to 10 are the theoretical limits, given by Voigt, Reuss and Hashin and Shtrikman, which govern the elastic moduli of two-phase materials. These theoretical curves were drawn by knowing the elastic moduli of the two end-members, i.e. pure polypropylene and pure $CaCO_3$. The 0% $CaCO_3$ samples provided the elastic moduli of pure polypropylene. The mean values of the respective elastic moduli of the various 0% samples were used and were found to be

$$K = 4.294 \times 10^9\,\text{Pa}$$

$$G = 1.439 \times 10^9\,\text{Pa}$$

$$E = 3.883 \times 10^9\,\text{Pa}$$

$$\sigma = 0.3493$$

The elastic moduli for $CaCO_3$ were given by Mason [8]

TABLE II Standard deviations of measurements

Modulus	Maximum standard deviation	Mean of the standard deviations
K	0.02 GPa	0.01 GPa
G	0.04 GPa	0.02 GPa
E	0.07 GPa	0.04 GPa
σ	0.004	0.002

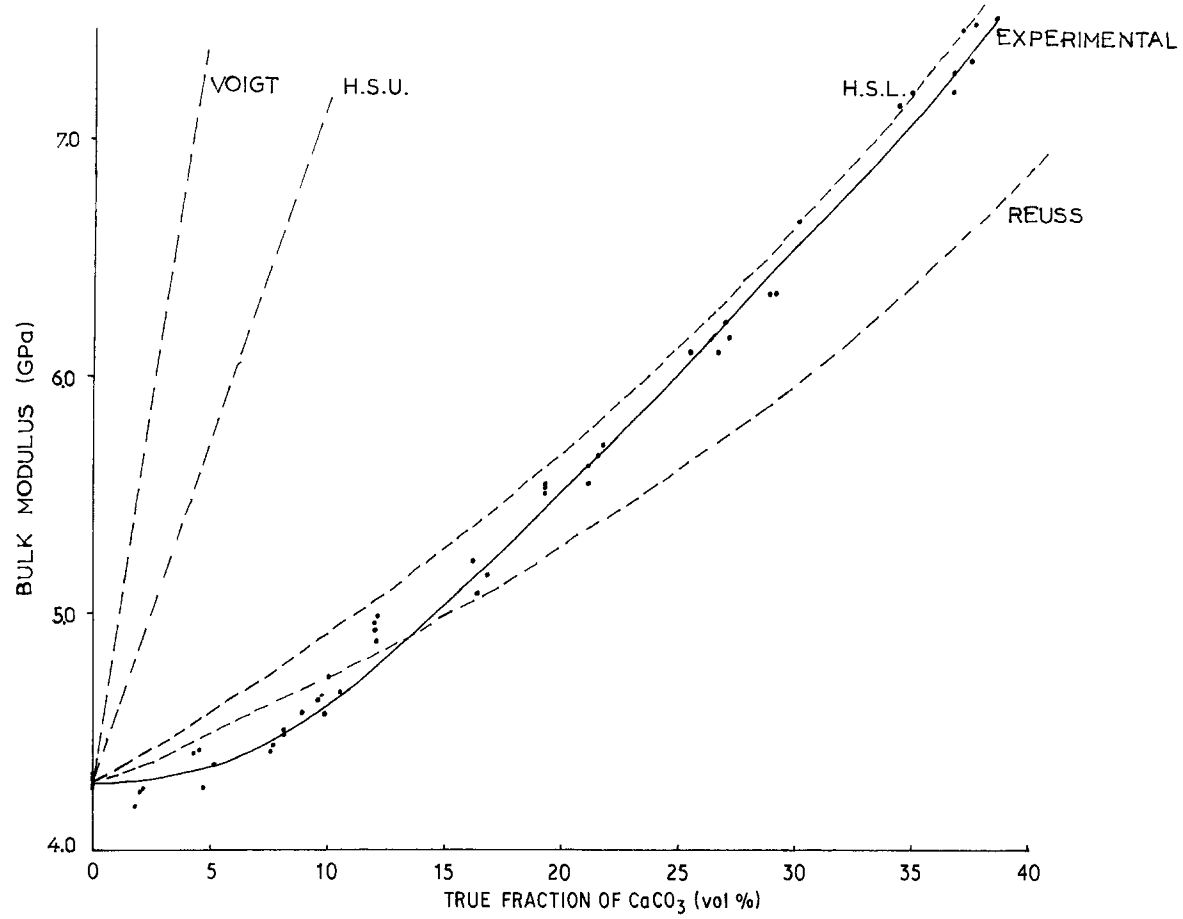

Figure 7 Composition dependence of bulk modulus. 'H.S.U.' and 'H.S.L.' denote Hashin and Shtrikman upper and lower bounds respectively.

as

$$K = 67.0 \times 10^9 \text{Pa}$$

$$G = 33.1 \times 10^9 \text{Pa}$$

It will be observed that the Hashin and Shtrikman bounds, although the narrowest that can be deduced without making special and specific assumptions about the phase geometry, are rather wide. This is because of the large ratio between the moduli of the pure matrix and pure filler phases. Nevertheless we have the striking results that all experimental values of all moduli lie close to the lower theoretical bound (upper bound in the case of Poisson's ratio). The agreement is better than 8% on average (and much better at the higher filler concentrations) even though the upper and lower bounds differ by several hundred

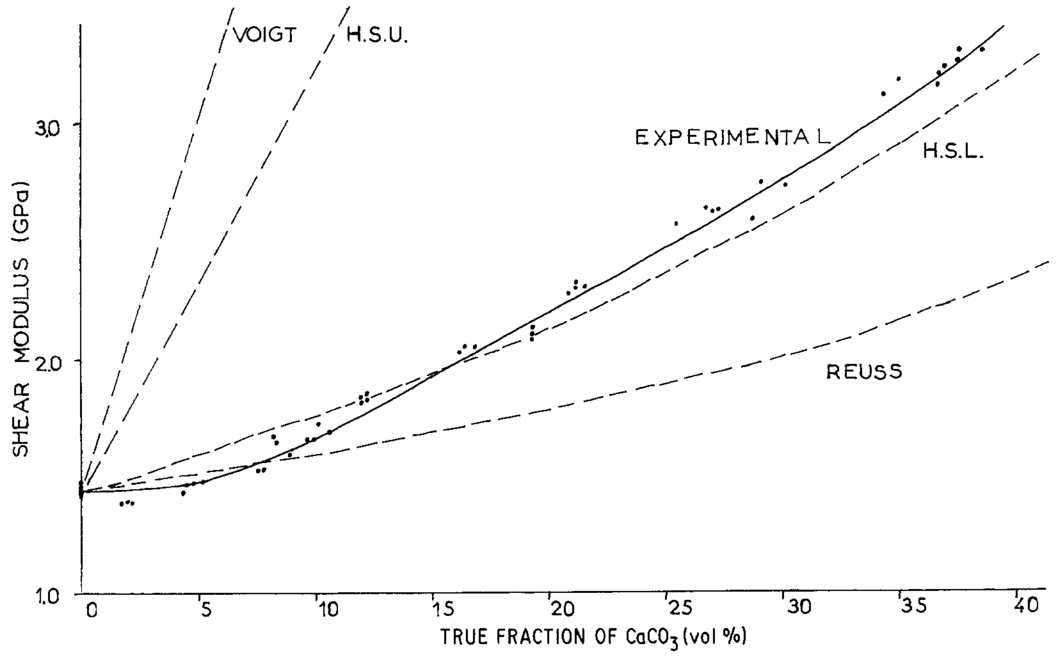

Figure 8 Composition dependence of shear modulus. 'H.S.U.' and 'H.S.L.' denote Hashin and Shtrikman upper and lower bounds respectively.

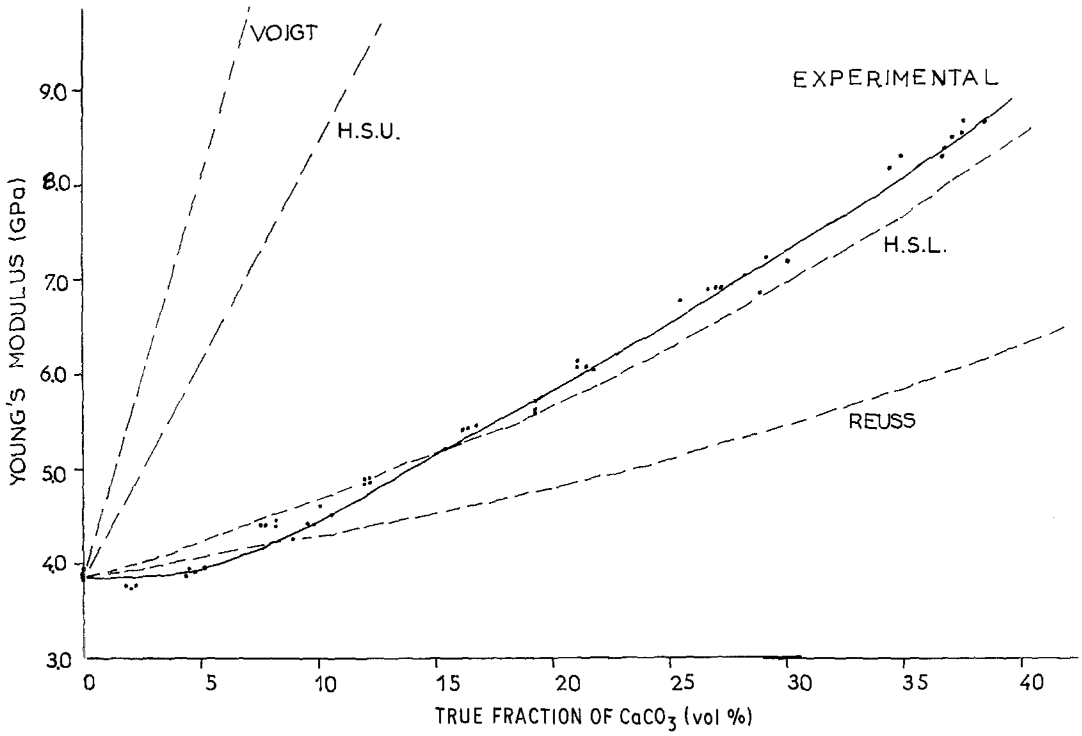

Figure 9 Composition dependence of Young's modulus. 'H.S.U.' and 'H.S.L.' denote Hashin and Shtrikman upper and lower bounds respectively.

per cent. Thus, from the arguments of Section 2 we conclude that the filler particles are (i) uniformly dispersed, (ii) are approximately or exactly spherical, (iii) are mostly of dimensions much less than $\lambda/4$ (which is about 100 μm for compressional waves), (iv) there are very few agglomerates or voids, (v) the filler–matrix bonding is consistent with the boundary conditions required of Hashin and Strickmanns' theory.

These views have been confirmed to a substantial degree by the use of another novel non-destructive technique. A microfocus radiograph of a 3 mm thick sample with 20% volume fraction of filler, was taken. The radiograph was taken using the first microfocus tube produced by Pantak Ltd [9], which has a state-of-the-art 10 μm focal spot – allowing individual filler particles of dimensions down to 10 μm to be observed under appropriate circumstances. Unfortunately the contrast in the radiograph was two poor for it to be reproducible in this paper. Work is in hand to produce improved radiographs in the future.

5. Conclusions

Our results are rather undramatic in that they have confirmed that the $CaCO_3$–polypropylene specimens produced were well-behaved ones. However, the precision of measurement achieved confirms the potential of this non-destructive technique for evaluating bulk quantities of poor, ill-fabricated materials.

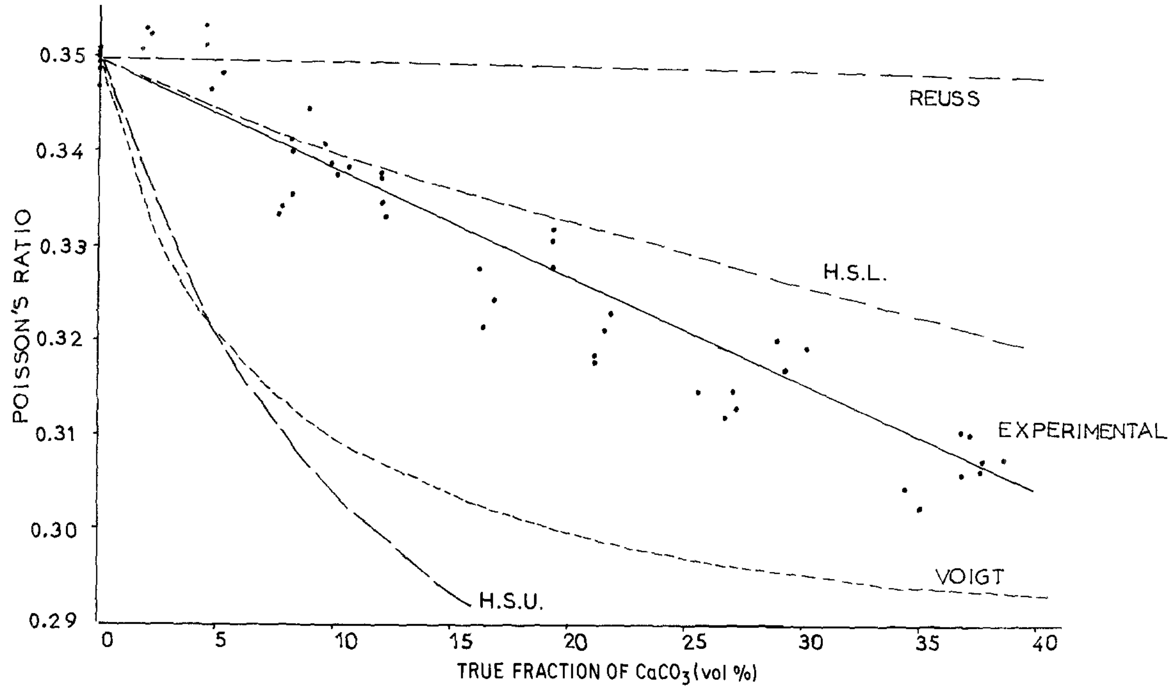

Figure 10 Composition dependence of Poisson's ratio. 'H.S.U.' and 'H.S.L.' denote Hashin and Shtrikman upper and lower bounds respectively.

Other more elaborate ultrasonic tests involving scattering experiments, for example, are planned to be performed on the same specimens.

Acknowledgements

Thanks are due to Professor M. E. Bevis and Dr P. Hornsby of the Materials Technology Department, Brunel University (for the provision of extrusion favilities) and to Dr P. McDonald, Project Manager, Microfocus Radiography, Astrophysics Research Ltd [13] for the exploratory microfocus radiography.

References

1. B. BRIDGE and P. ISMAIL, "Nondestructive Testing Communications" (Gordon and Breach, New York, (1984) pp. 155–164.
2. B. BRIDGE, A. PERSEH and P. S. ALLAN, *J. Mater. Sci. Lett.* **6** (1987) 81.
3. Z. HASHIN, *J. Appl. Mech.* **29** (1962) 143.
4. Z. HASHIN and S. SHTRIKMAN, *J. Mech. Phys. Solids* **11** (1963) 127.
5. R. SHAW and D. UHLMANN, *J. Non-Cryst. Solids* **5** (1971) 237.
6. B. BRIDGE and A. A. HIGAZY, *J. Mater. Sci.* **20** (1985) 4484.
7. B. BRIDGE, in Proceedings of Symposium on Non-destructive Measurement of Material Properties of Fitness for Service, May 1984 (British Institute of Non-Destructive Testing, Northampton NN1 5AA, UK) p. 2.
8. C. M. SAYERS and R. L. SMITH, *J. Phys. D* **16** (1983) 1189.
9. C. M. SAYERS and C. E. TAIT, *Ultrasonics* **22** (1984) 57.
10. A. A. HIGAZY and B. BRIDGE, *J. Non-Cryst. Solids* **72** (1985) 81.
11. N. D. PATEL, B. BRIDGE and D. N. WATERS, *Phys. Chem. Glasses* **24** (5) (1983) 122.
12. B. BRIDGE and N. D. PATEL, *J. Mater. Sci.* **21** (1986) 1187.
13. P. McDONALD, Private communication, (1986), Astrophysics Research Ltd, Vale Road, Windsor, Berkshire SL4 5JB, UK.

Received 25 July
and accepted 22 September 1986